Active loss mitigation and modes in an artificial material made of a 3D-lattice of plasmonic nanoshells

S. Campione[1], M. Albani[2], F. Capolino[1]

[1]Department of Electrical Engineering and Computer Science, University of California, Irvine
92697–2625 Irvine, CA, USA
Fax: +1–949–824–1853; email: scampion@uci.edu ; f.capolino@uci.edu
[2]Department of Information Engineering, University of Siena
53100, Siena, Italy
Fax: +39–0577–233609; email: matteo.albani@dii.unisi.it

Abstract

We show a study of complex modes and loss compensation at plasmonic frequencies of 3D-periodic arrays of metallic core – dielectric shell nanospheres embedded in a homogeneous background. Each nanoshell is modeled as an electric dipole through single dipole approximation, the metal permittivity is model by using the Drude model and the complex modes are computed by means of the 3D-periodic dispersion relation. Active gain materials are introduced in the dielectric shell to compensate the intrinsic losses of the metal and thus at optical frequencies. The effective refractive index versus frequency obtained by the modal analysis with and without loss compensation is shown and compared to that obtained by Maxwell Garnett homogenization theory.

1. Introduction

3D-periodic arrays of nanospheres can be engineered to obtain peculiar characteristics, such as slow wave structures and double negative materials. The usage of nanoshell particles allows, by varying the relative dimensions of the core and the shell, the tuning of their optical resonance over hundreds of nanometers in wavelength, across the visible and into the infrared region of the spectrum. In addition, active gain materials can be introduced into the nanoshell's dielectric region to mitigate the intrinsic losses of the metal at optical frequencies. Mode analysis and optical properties of 3D-periodic arrays of nanoshells have been analyzed in [1-2]. Usage of gain materials in nanoshells has been shown in [3]. In this paper, we analyze the complex modes in the 3D-periodic arrays of metallic core – dielectric shell nanospheres in Fig. 1 for transversal (with respect to the mode traveling direction, T-pol) polarization. We then analyze the use of an active gain material to overcome the metallic losses of the metamaterial. The effective refractive index obtained by the modal analysis for transverse polarization is compared to that obtained by Maxwell Garnett homogenization theory [4].

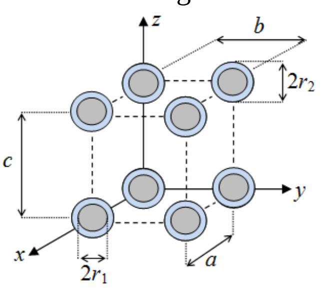

Fig. 1: 3D-periodic array of metallic core – dielectric shell nanospheres embedded in a homogeneous medium with permittivity ε_h. The core and the shell radius are r_1 and r_2, respectively; *a*, *b* and *c* are the periodicities along *x*-, *y*- and *z*-direction, respectively.

2. Mode analysis and active gain material modeling

Single dipole approximation (SDA) [5] is adopted to model each nanoshell to act as an electric dipole in the case of small nanoshells (with respect to the wavelength) close to their plasmonic resonance fre-

ISBN 978-952-67611-0-7

quency. According to SDA, the induced dipole moment is $\mathbf{p} = \alpha_{ee}\mathbf{E}^{loc}$, with α_{ee} being the electric polarizability of the nanoshell (we adopt the quasistatic approximation including dipole radiation correction [6-8]), and $\mathbf{E}^{loc}$ is the local field produced by all the nanoshells of the array except the considered nanoshell plus the external incident field to the array. Complex modes in 3D arrays are then found by using the procedure outlined in [5]. The linear active constitutive relation (relative permittivity) for a 4-level atomic transition active gain material in the time harmonic regime can be expressed as [9]

$$\varepsilon_g = \varepsilon_r + \frac{\sigma_a}{\left[\omega^2 + i\Gamma_a\omega - \omega_a^2\right]} \frac{\left(\tau_{21} - \tau_{10}\right)\Gamma_{pump}}{\left[1 + \left(\tau_{32} + \tau_{21} + \tau_{10}\right)\Gamma_{pump}\right]} \frac{\bar{N}_0}{\varepsilon_0}, \quad (1)$$

where Γ_a is the bandwidth of the atomic transition at angular frequency ω_a, τ_{ij} is the non-radiative decay lifetime from the *i*-th to the *j*-th energy level, $\bar{N}_0$ is the total electron density, and Γ_{pump} is the pumping rate. Also, we assume that the gain material is embedded into a dielectric material with permittivity ε_r (i.e., the dielectric shell here).

3. Dispersion diagrams and effective refractive index

We analyze the complex modes traveling along the *z*-direction in a 3D-periodic array of nanoshells in free space (i.e., $\varepsilon_h = 1$), for T-pol, accounting for metal losses and also for the ideal lossless case (γ = 0 in the Drude model for the metal). The dielectric shell is assumed to have a permittivity as in (1), and the hosting dielectric material is glass with $\varepsilon_r = 2.25$. The values of the parameters in (1) are assumed to be equal to those in [9]: $\Gamma_a = 2\pi \times 20 \times 10^{12}$ rad/s, $\sigma_a = 10^{-4}$ C^2/kg, $\tau_{32} = 50$ fs, $\tau_{21} = 5$ ps, $\tau_{10} = 50$ fs, $\bar{N}_0 = 5 \times 10^{23}$ m^{-3}. The nanoshell parameters are $r_2 = 25$ nm, $\rho = r_1/r_2 = 0.8$. The core is made of silver, whose Drude parametes are [10]: $\varepsilon_\infty = 5$, $\omega_p = 1.37 \times 10^{16}$ rad/s, and $\gamma = 27.3 \times 10^{12}$ s^{-1}. We assume a cubic lattice with $a = b = c = 75$ nm, thus the filling factor is $f = 4\pi r_2^3/(3a^3) = 0.155$. The dispersion diagrams for the structure in Fig. 1, accounting for losses and for the lossless ideal case, are shown in Fig. 2 (we focus only on the dominant mode). The lossless curve represents the best that could be achieved with a loss compensation mechanism. The plasmonic resonance of the nanoshells in the 3D lattice are the cause of the strong dispersion around $ka/\pi \approx 0.4$. Loss compensation can be performed at frequencies right before or after the strong dispersion, as highlighted in Fig. 2(b) by the black circle, where the refractive index is high or low (less than unity).

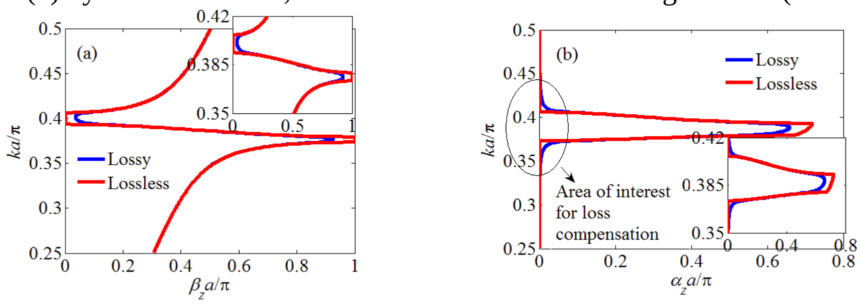

Fig. 2: Dispersion diagram for T-pol, for lossless and lossy metal. (a) Real part and (b) imaginary part of the wavenumber k_z. k is the background wavenumber, and here coincides with the free space wavenumber.

As an example we show the effect of the gain material in the frequency region right after the strong dispersion where the effective refractive index is low, Fig. 3. There, increasing frequency, the effective permittivity passes from negative to positive values, both being near zero. As an example, we choose an active gain emission center frequency $f_a = \omega_a/(2\pi) = 812$ THz ($ka/\pi = 0.406$) overlapping with the interested frequency region and apply a constant pumping rate $\Gamma_{pump} = 1.65 \times 10^9$ s^{-1} (a higher value would cause overcompensation of the losses). It can be observed in Figs. 3(a) and 3(b) that the black curve (Modes – with gain) tends to recover the ideal result represented by the red curve (Modes – lossless) around the emission peak frequency of the gain material. The result obtained from the mode analysis is compared with that obtained with the Maxwell Garnett (MG) method which provided the effective permittivity. In Fig. 3(b) one can notice that the MG analysis provides the same conclusion about loss compensation, except for an expected frequency shift with respect to the mode analysis. The figure of merit, or $\mathrm{FOM} = \mathrm{Re}[n^{\mathrm{eff}}] / \mathrm{Im}[n^{\mathrm{eff}}]$, shown in Fig. 3(c), has been conspicuously improved, because losses have been partly compensated.

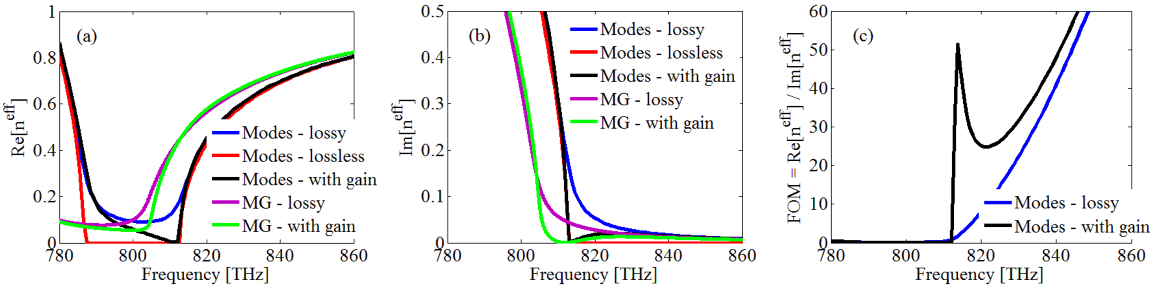

Fig. 3: (a) Real part and (b) imaginary part of the effective refractive index computed by means of the 3D-periodic dispersion relation (Modes) and the Maxwell Garnett approximation (MG) for the compensation after the strong dispersion. (c) Figure of merit.

4. Conclusion

We have shown that active gain materials can be adopted to overcome metallic losses at optical frequencies; the effectiveness of such a compensation has been shown in region right after the strong dispersion of the computed complex modes, comparing results from modal analysis and Maxwell Garnett formulation. Metamaterials with near-zero refractive index can be designed with losses almost totally compensated.

Acknowledgment – This work has been partly funded by the European Union's FP7-NMP-2008 program under the METACHEM project (grant n° 228762).

References

[1] J. Li, G. Sun and C.T. Chan, Optical properties of photonic crystals composed of metal-coated spheres, *Physical Review B*, vol. 73, p. 075117, 2006.
[2] C. Tserkezis, G. Gantzounis and N. Stefanou, Collective plasmonic modes in ordered assemblies of metallic nanoshells, *Journal of Physics-Condensed Matter*, vol. 20, p. 075232, 2008.
[3] M.I. Stockman, The spaser as a nanoscale quantum generator and ultrafast amplifier, *Journal of Optics*, vol. 12, p. 024004, 2010.
[4] R. Ruppin, Evaluation of extended Maxwell-Garnett theories, *Optics Communications*, vol. 182, pp. 273-279, 2000.
[5] S. Steshenko and F. Capolino, Single Dipole Approximation for Modeling Collection of Nanoscatterers, in *Theory and Phenomena of Metamaterials*, F. Capolino, ed., Boca Raton, FL, CRC Press, 2009.
[6] C.F. Bohren and D.R. Huffman, *Absorption and Scattering of Light by Small Particles*, New York, Wiley, 1983.
[7] K. Tanabe, Field enhancement around metal nanoparticles and nanoshells: A systematic investigation, *Journal of Physical Chemistry C*, vol. 112, pp. 15721-15728, 2008.
[8] A. Vallecchi, S. Campione and F. Capolino, Symmetric and antisymmetric resonances in a pair of metal-dielectric nanoshells: tunability and closed-form formulas, *Journal of Nanophotonics*, vol. 4, p. 041577, 2010.
[9] A. Fang, T. Koschny, M. Wegener and C.M. Soukoulis, Self-consistent calculation of metamaterials with gain, *Physical Review B*, vol. 79, p. 241104, 2009.
[10] I. El-Kady, M.M. Sigalas, R. Biswas, K.M. Ho and C.M. Soukoulis, Metallic photonic crystals at optical wavelengths, *Physical Review B*, vol. 62, p. 15299, 2000.